Editors' Suggestion

# Test of Local Realism into the Past without Detection and Locality Loopholes

Ming-Han Li,[1,2] Cheng Wu,[1,2] Yanbao Zhang,[3] Wen-Zhao Liu,[1,2] Bing Bai,[1,2] Yang Liu,[1,2] Weijun Zhang,[4] Qi Zhao,[5] Hao Li,[4] Zhen Wang,[4] Lixing You,[4] W. J. Munro,[3] Juan Yin,[1,2] Jun Zhang,[1,2] Cheng-Zhi Peng,[1,2] Xiongfeng Ma,[5] Qiang Zhang,[1,2] Jingyun Fan,[1,2] and Jian-Wei Pan[1,2]

[1]*Shanghai Branch, National Laboratory for Physical Sciences at Microscale and Department of Modern Physics, University of Science and Technology of China, Shanghai 201315, People's Republic of China*

[2]*Shanghai Branch, CAS Center for Excellence and Synergetic Innovation Center in Quantum Information and Quantum Physics, University of Science and Technology of China, Shanghai 201315, People's Republic of China*

[3]*NTT Basic Research Laboratories and NTT Research Center for Theoretical Quantum Physics, NTT Corporation, 3-1 Morinosato-Wakamiya, Atsugi, Kanagawa 243-0198, Japan*

[4]*State Key Laboratory of Functional Materials for Informatics, Shanghai Institute of Microsystem and Information Technology, Chinese Academy of Sciences, Shanghai 200050, People's Republic of China*

[5]*Center for Quantum Information, Institute for Interdisciplinary Information Sciences, Tsinghua University, Beijing 100084, People's Republic of China*

(Received 9 April 2018; revised manuscript received 11 June 2018; published 20 August 2018)

Inspired by the recent remarkable progress in the experimental test of local realism, we report here such a test that achieves an efficiency greater than $(78\%)^2$ for entangled photon pairs separated by 183 m. Further utilizing the randomness in cosmic photons from pairs of stars on the opposite sides of the sky for the measurement setting choices, we not only close the locality and detection loopholes simultaneously, but also test the null hypothesis against local hidden variable mechanisms for events that took place 11 years ago (13 orders of magnitude longer than previous experiments). After considering the bias in measurement setting choices, we obtain an upper bound on the $p$ value of $7.87 \times 10^{-4}$, which clearly indicates the rejection with high confidence of potential local hidden variable models. One may further push the time constraint on local hidden variable mechanisms deep into the cosmic history by taking advantage of the randomness in photon emissions from quasars with large aperture telescopes.

DOI: 10.1103/PhysRevLett.121.080404

It has long been known that many of the predictions of quantum mechanics are counterintuitive and are strictly prohibited by local realism, our usual model of the world. This led to the famous question "Can a Quantum-Mechanical Description of Physical Reality be Considered Complete?" by Einstein *et al.* in 1935 [1]. Local realism requires that a system possesses an exact property prior to its measurement and the cause-effect action is limited by the speed of light. Quantum mechanics on the other hand presents a different description of our world, by allowing the presence of quantum superposition and nonlocal correlations between distant entangled particles. These nonlocal quantum mechanical correlations provide predications incompatible with local realism. John Bell introduced his celebrated inequality for a definitive hypothesis test of local realism to end the dispute [2,3].

Bell considered that the two parties Alice and Bob make a joint measurement on their remotely separated entangled particles. For measurement setting choices $x$, $y \in \{0, 1\}$, they receive the measurement outcomes $a$, $b \in \{0, 1\}$, respectively. According to local hidden variable models, the outcomes $a$ and $b$ are completely (pre)determined for the inputs $x$, $y$ and a hidden variable $\lambda$ carrying the exact state information such that $a = a(x, \lambda)$ and $b = b(y, \lambda)$. Local hidden variable models set a bound on the joint measurement probability distribution $p(a, b|x, y, \lambda)$, while quantum mechanical predictions surpass this bound [2–5]. The experimental violation of the Bell inequality was observed shortly after its derivation and is now routinely performed in quantum physics laboratories (see [6–8] for a recent review). However, the imperfections in experiments open loopholes for local hidden variable theories to reproduce the observed violation of Bell inequality, which would otherwise be a strong evidence against local realism.

The detection of entangled particles in a Bell test experiment can be corrupted by loss and noise. The consequence of this is that the ensemble of the detected states may not be an honest representative of what the source actually emits. It was shown that the local hidden variable models can explain the observed violation of Bell inequality if the detection efficiency of single entangled particles is $\leq 2/3$ [9], which is known as the detection (fair sampling) loophole [10]. The Bell test experiment requires one to separate the measurement setting choice and measurement outcome on one side spacelike from the measurement setting choice on the other. Failure to do so opens the locality loophole [11], which allows the two parties to communicate about their measurement settings

 

before outputting outcomes. Further, the Bell test experiment also requires the measurement setting choices to be "truly free or random" and that "they are not influenced by the hidden variables" [3]. The light cones of the measurement events on both sides and the entanglement creation at the source in a Bell test experiment cross each other in the past direction. A hidden cause in the common past can manipulate the experimental outcomes in the Bell test experiment, opening the freedom-of-choice loophole [3].

The experimental test of Bell inequality was pioneered by Freedman and Clauser [12] and Aspect *et al.* [13–15]. The locality and detection loopholes were individually closed initially by Aspect *et al.* [15], Weihs *et al.* [16], and Rowe *et al.* [17], followed by a number of others [18–21]. Scheidl *et al.* made the first attempt on the freedom-of-choice loophole [22]. Several groups have recently succeeded in closing both locality and detection loopholes simultaneously in Bell test experiments [23–26]. Spacetime analysis shows that the common past in these experiments [24,25] began by less than $<10^{-5}$ s before the experiment. We denote this time as $t_{cm}$, with $t_{cm} = -10^{-5}$ s with respect to the starting time of the Bell experiment. The outcomes in these experiments are possibly subject to the influence of local hidden variable models taking place before $t_{cm}$. In this Letter, we report on achieving $t_{cm} = -11$ yr by using the randomness in cosmic photons for measurement setting choices in a Bell test experiment. With both detection and locality loopholes closed, and considering the distribution bias in measurement settings observed in the experiment, the prediction-based ratio (PBR) analysis method [27–29] produces a $p$ value upper bound for the null hypothesis test to be $\leq 7.873 \times 10^{-4}$, indicating a rejection of local hidden variable models taking place after $t_{cm} = -11$ yr with high confidence.

Shown from our experimental layout depicted in Fig. 1, we create entangled photon pairs at 1560 nm by a spontaneous parametric down-conversion process periodically at a repetition rate of 2 MHz and distribute the two photons of each pair via single mode optical fiber in opposite directions to Alice and Bob, which are at a distance of 93 and 90 m from the source, respectively. At each measurement station, the entangled photons exit the fiber and pass through a Pockels cell for the polarization state measurement. They are then coupled into the single mode optical fiber to be detected by the superconducting nanowire single-photon detectors [30]. The heralding efficiency of single photons, from creation to detection, is obtained as the ratio of the two-photon coincident counting events with respect to the single-photon counting events, which is $(78.8 \pm 1.9)\%$ for Alice and $(78.7 \pm 1.5)\%$ for Bob in the experiment [31,32], and is sufficient to close the detection loophole. We measure a two-photon quantum interference visibility of 99.4% in the horizontal (vertical) base and 98.4% in the diagonal (anti-diagonal) base. Further, we obtain a fidelity of 98.66% in the quantum state tomography measurement, with which we numerically find the nonmaximally polarization-entangled state, $\cos(22.05°)|HV\rangle + \sin(22.05°)|VH\rangle$. With the measurement settings [$-83.5°$ (for $x = 0$) and $-119.4°$ (for $x = 1$) for Alice, and $6.5°$ (for $y = 0$) and $-29.4°$ (for $y = 1$) for Bob], we obtain an optimum violation of the Bell inequality [9] (see Supplemental Material for the detailed description of quantum state characterization [33]).

Because of the presence of a common past, one can only test against local hidden variable models taking place after $t_{cm}$ in a Bell test experiment. Bell and a few others considered to use the randomness generated long before the experiment in the Universe to make $t_{cm}$ significantly large in the past direction [22,34–36]. Employing the randomness in certain properties of cosmic photons such as the arrival time, color, and polarization for the measurement setting choice in a Bell experiment has attracted significant recent attention [37–40]. Here, we present a Bell test experiment employing the randomness in the creation time of cosmic photons. Therefore, the arrival times of a pair of cosmic photons, which are respectively emitted by a pair of cosmic sources located on the opposite sides of our sky, are random and so can be used for Alice's and Bob's measurement setting choices. To do so, at each measurement station, we use a telescope (Celestron, CPC 1100 HD) to receive photons from the selected cosmic radiation source, which has a diameter of 280 mm and a focal length of $f = 2.94$ m. We use a beam splitter to reflect a portion of the collected cosmic photons to form an image of the cosmic source on a CCD camera (Andor Zyla, $2048 \times 2048$ pixels with a pixel size of 6.5 $\mu$m) and couple the transmitted photons into a multimode fiber with NA $= 0.22$ and a core diameter of 105 $\mu$m, which is connected to a silicon single-photon avalanche diode (SPAD). We estimate the total detection efficiency of a single cosmic photon within the spectral band of silicon SPAD to be $<1\%$ [39]. Both the sensitive area of the CCD camera and the fiber end facet are at the focal plane of the telescope. The intensity profile of the image of the cosmic source is used in a tracking mechanism to stabilize the coupling of photons from the cosmic source into the fiber during the experiment [41]. We pass the cosmic photon detection signals from the SPAD to a field programmable gate array (FPGA), which converts the random arrival time of cosmic photons into random bits for our Alice and Bob measurement setting choices.

The spacetime diagram of our experiment is presented in Fig. 2 beginning with the event of creating a state in the source (at a repetition rate of 2 MHz) as the origin. To ensure that the measurement setting choice of the Alice (Bob) measurement is spacelike separated from the measurement process of the Bob (Alice) measurement, we require that, when a cosmic photon from the selected cosmic source arrives at the telescope of Alice (Bob), its wave front has not arrived before Bob (Alice) finishes his (her) state measurement, which is quantified by two

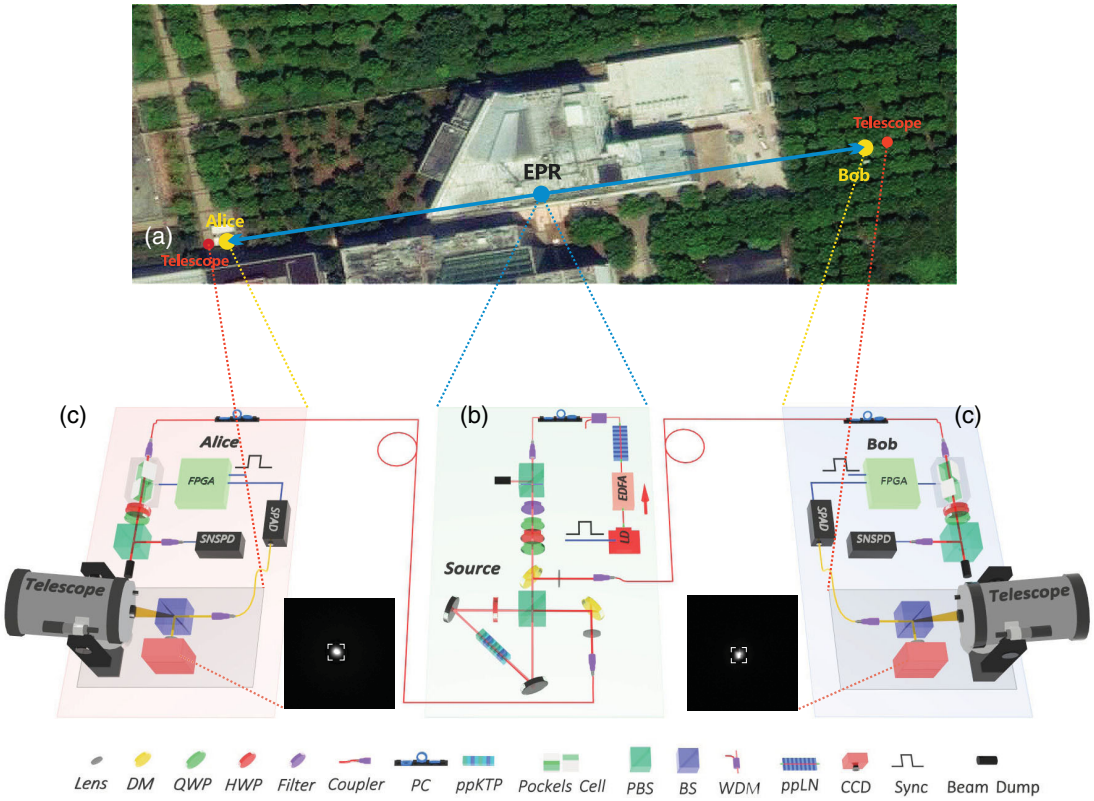


FIG. 1. Experimental schematics. (a) A bird's-eye view of the experimental layout. Alice's and Bob's measurement stations are on the opposite sides of and, respectively, $93 \pm 1$ and $90 \pm 1$ m from the entangle photon pair source (labeled by EPR in the figure). Both Alice and Bob have a telescope 3 m from the measurement station to collect cosmic photons. (b) Creation of pairs of entangled photons: light pulses of 10 ns, 2 MHz from a 1560 nm seed laser diode (LD) are amplified by an erbium-doped fiber amplifier (EDFA) and frequency-doubled in an in-line periodically poled lithium niobate (PPLN) crystal. With the residual 1560 nm light removed by a wavelength-division multiplexer (WDM) and spectral filters, the 780 nm light pulses are focused into a periodically poled potassium titanyl phosphate (PPKTP) crystal in a Sagnac loop to generate polarization entangled photon pairs. A set of quarter-wave plates (QWPs) and a half-wave plate (HWP) are then used to control the relative amplitude and phase in the created polarization-entangled two-photon state. The residual 780 nm pump light is removed by dichroic mirrors (DMs). The two photons of an entangled pair at 1560 nm travel through optical fiber in opposite directions to two measurement stations, where they are subject to polarization state measurements. (c) Single photon polarization state measurement: the single photons exit the fiber, go through the polarization state measurement in free space, and are collected into a single mode optical fiber to be detected by superconducting nanowire single-photon detectors (SNSPDs). The apparatus to perform single-photon polarization measurement consists of a Pockels cell, QWP, HWP, and polarizing beam splitter (PBS). The cosmic photons collected by the telescope are split by a beam splitter (BS). The transmitted photons are coupled into the optical fiber and detected by a SPAD. The reflected photons form an image on a CCD camera, which is used for star tracking and stabilizing the coupling of cosmic photons into optical fiber. The SPAD outputs are fed to a FPGA to generate random bits for measurement setting choice to trigger the Pockels cell to switch between two polarization orientations. A time-to-digital converter (TDC) is used to time tag the events of cosmic random number generation and single-photon detection (see Supplemental Material [33] for detailed experimental setup, which includes Ref. [30]). (Insets) Star images (HIP 43813 and HIP 86032, respectively, for Alice and Bob) on the CCD camera for star tracking.

parameters, $\Gamma^A$ and $\Gamma^B$, respectively. Having $\Gamma^A > 0$ and $\Gamma^B > 0$ means we satisfy the spacelike separation condition (see Supplemental Material [33] for details about the derivation of $\Gamma^A$ and $\Gamma^B$, which includes Refs. [42–44]). In our experiment with the available choices of stars, by setting the time window to accept the cosmic photons to be 133.2 ns, we have $\Gamma^A > 58$ ns and $\Gamma^B > 60$ ns (as shown in Table I). It is important to note here that we only consider the optical refraction effect due to the atmosphere of Earth and assume that the interstellar space is vacuum in the current spacetime analysis. The interstellar medium has extremely low density [45–48]. It will be interesting to consider the possible delay of light propagation due to the interstellar medium in the future when the precise relevant information is available. Here, we assume that the propagation of cosmic photons and their arrival time are not affected by any means other than the known mechanisms in astronomy studies, such as refraction through slowly varying interstellar medium, and assume the effect is identical for all photons.

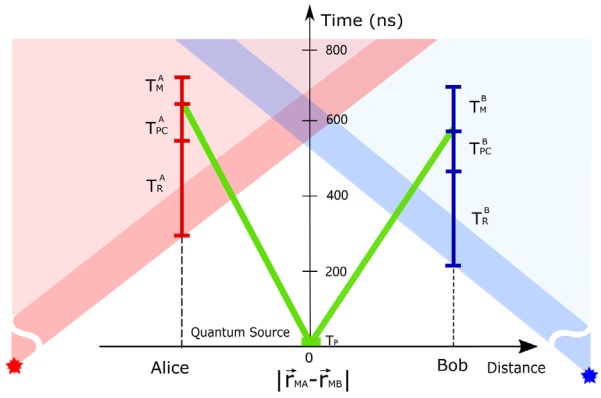


FIG. 2. Spacetime diagram of the Bell test experiment. The green dot represents the event of creating an entangled photon pair in the source, while the two thick green lines stand for delivering the photons to Alice and Bob via optical fiber, both having an uncertainty of 10 ns, which is the temporal duration of the pump laser pulse. For Alice's (Bob's) side, the red (blue) line segments labeled by $T_R^A$ ($T_R^B$), $T_{\mathrm{PC}}^A$ ($T_{\mathrm{PC}}^B$), and $T_M^A$ ($T_M^B$) represent the time elapse starting from cosmic photons arriving at the telescope to the Pockels cell receiving a random bit, then to an entangled single photon leaving the Pockels cell, then to the photon detection circuit outputting a signal. The red (blue) strip stands for the time window to accept the cosmic photons for random bit generation, satisfying the spacelike separation condition through the entire duration of the experiment.

We use a master clock to produce synchronization signals at a repetition rate of 2 MHz, which is used to trigger the source to produce states. It further serves as an external clock to the FPGA. We convert the random arrival time of a cosmic photon received in the time window into a 1-bit random number in the following simple way: if a photon-detection signal from the SPAD is within 133.2 ns before a clock signal (at 2 MHz) in the FPGA, the FPGA outputs a random bit 0 if the photon-detection signal appears in the first 66.6 ns, while if the photon-detection signal appears in the second 66.6 ns window, the FPGA outputs a random bit 1. The FPGA does not output random bits in the following 5 $\mu$s, instead it applies an artificial 5 $\mu$s dead time (see Supplemental Material for detailed description of synchronization and random number generation with cosmic photons [33]). This cosmic random number generator outputs random bits at a rate not exceeding 200 000 $\mathrm{s}^{-1}$, which is the maximum rate the Pockels cells can be switched at to realize the measurement settings in the current experiment. We now define an experimental trial as the case when both cosmic random number generators on the two sides simultaneously produce a random bit.

The local conditions, such as the weather (humidity, atmospheric turbulence, temperature variation), tall buildings, and light pollution, besides the sky glow in Shanghai, permit us to select only among a few stars of low magnitude with our 280 mm telescopes for the experiment. Because of Earth's rotation and the time spent on finding the stars and optimizing the coupling of stellar photons into the fiber, we did the experiment with a pair of stars selected for Alice and Bob for about 10–40 mins and then chose another pair of stars to continue the experiment. We conservatively set $t_{cm} = -11.46$ yr (see Table I). The signal-to-noise ratio of the produced random numbers ranges from 78 to 584. The noise is taken by pointing the telescope slightly away from the cosmic source (at a dark patch of the sky). We notice that the ratio of the frequency of bit 1 with respect to that of bit 0 deviates slightly from the ideal value of 1, which may be due to the system imperfections, including single-photon detector dead time and the time window broadening due to processing the detection of multiphotons in the FPGA [49], which will be further optimized in future work.

Noting that we have achieved high single-photon detection efficiency and ensured spacelike separation between relevant events, we now illustrate that we indeed close loopholes in our Bell test experiment, particularly the detection loophole, which has two related issues. One is related to the loss of entangled photons from creation to detection due to the system imperfection, and the other is related to the inefficiency in detecting cosmic photons. From a pedagogical perspective, we present the discussion with a general nonlocal game, where the two stars can be

TABLE I. Key parameters in the Bell test experiment. In each experimental run, we select a pair of stars with one for Alice and one for Bob, find the smallest $t_{cm}$ and $\Gamma_{A(B)}$ considering Earth's rotation, list the start time (UTC time) and run time [44], the ratio between the number of random number "0" and the number of random number "1" (0/1), signal-to-noise ratio (SNR), and the calculated bias $\delta\Gamma_{A(B)} = 4$ ns.

| Run | | HIP ID | Start (UTC) time | Run time(s) | $t_{cm} \pm \delta_{t_{cm}}$ (yr) | $\Gamma_{A(B)}$ | 0/1 | SNR | Bias |
|---|---|---|---|---|---|---|---|---|---|
| 1 | Alice | 21421 | 2018/3/23 13 h 34 min | 416 | $-36.71 \pm 0.22$ | 144 | 1.0078 | 491.6 | 0.002 95 |
| | Bob | 69673A | | | | 69 | 1.0012 | 94.7 | 0.005 52 |
| 2 | Alice | 27989 | 2018/3/23 14 h 14 min | 2026 | $-75.03 \pm 3.73$ | 155 | 1.0053 | 584.6 | 0.002 17 |
| | Bob | 76267 | | | | 60 | 0.9989 | 111.6 | 0.004 71 |
| 3 | Alice | 37279 | 2018/3/23 15 h 13 min | 2638 | $-11.46 \pm 0.05$ | 105 | 1.0059 | 147.4 | 0.004 83 |
| | Bob | 80816 | | | | 58 | 0.9985 | 78.5 | 0.006 66 |
| 4 | Alice | 43813 | 2018/3/23 16 h 26 min | 2330 | $-48.58 \pm 0.77$ | 99 | 1.0009 | 125.2 | 0.004 19 |
| | Bob | 86032 | | | | 71 | 0.9987 | 132.6 | 0.004 07 |

regarded as two referees. In each trial of the game, Alice and Bob, as two players who are not allowed to communicate during the trial, each receives a 1-bit random number as the input $x$ and $y$ and outputs a 1-bit outcome $a$ and $b$, respectively. The score for each trial is calculated according to the inputs and outputs. We stress that, in each trial of the game, both referees give random bits, and the detection loophole problem arises when one or both players do not always have outputs (say, due to channel loss). In this case, Alice and Bob can prepare some (input and output) bits ahead and, if their input bits match the referees, they would output the corresponding output bits, and they would not provide outputs if the input bits are not matched. Such detection loophole was well studied in the past, which can be closed with high single-photon detection efficiency. On the other hand, it is okay that one or both referees sometimes do not want to play and therefore do not provide random bits in the game. We stress that it is not counted as a game trial when this happens, and it is counted as a game trial if and only if both referees provide random numbers at both sides. Hence, such cases do not introduce the detection loophole. We remark that similar treatments have already been employed, e.g., in the spot-checking device-independent protocol [50,51], in which only a small fraction of trials are randomly selected as test trials for the loophole-free Bell test, but the security of an information task based on other trial results is guaranteed.

We quantify the small bias in the generated random bits distribution by the total-variance distance from the uniform distribution. Because it is impossible to fully characterize this bias, we make the assumption that the random bits distribution bias at each measurement station in each trial is bounded to and independent of each other. We remark that under this situation we allow the measurement dependence, i.e., the dependence of the distribution of input random numbers at each measurement station on the local hidden variables as studied in Refs. [52–54]. We also allow the possibility that the distribution bias changes from trial to trial, and our data analysis method can take advantage of the knowledge of the bias change over time. The evidence against the null hypothesis of local realism, under the above assumption, is quantified in a reference computed using test statistics. The $p$ value is the maximum probability according to local realism that the statistics take a value as extreme as the observed one. Hence, a small $p$ value implies a strong evidence against local realism. We apply the PBR analysis method in designing the test statistics and computing an upper bound of the $p$ value. The PBR analysis was originally developed for the test of local realism, assuming that the input measurement setting distribution is fixed and known [28,29], and later extended to the case with a relaxed assumption that the setting distribution bias is bounded [27]. Hence, the PBR analysis method can be applied to our current situation. The PBR analysis provides valid upper bounds of $p$ values, even if the local realistic models depend on previous trial results and the experimental distribution of trial results varies over time. The bias in random bit distribution varies for different stars under the study, as shown in Table I. The PBR analysis incorporating the time-varying bias returns a $p$ value upper bound of $p = 7.873 \times 10^{-4}$. If we make a stronger but unjustified assumption that the measurement setting distribution is perfectly uniform, the PBR analysis returns a smaller $p$ value upper bound $p' = 3.106 \times 10^{-10}$ (see Supplemental Material for a detailed description of the PBR analysis method [33], which includes Refs. [27–29,55–59]). Both indicate a rejection of the assumed local hidden variable models with high statistical confidence. Compared with the recent loophole-free Bell tests reported in [23–26], our $p$ value upper bounds are larger than the $p$ value of $3.74 \times 10^{-31}$ in [25] or $2.57 \times 10^{-9}$ in [26] and are comparable to the $p$ value from $5.9 \times 10^{-3}$ to $9.2 \times 10^{-6}$ in [24], but smaller than the $p$ value of 0.019 in [23].

In conclusion, we perform a null hypothesis test that rejects local hidden variable models taking place as early as 11 years before the experiment with high confidence. Looking into the future, our experiment may serve as a benchmark to progressively rule out local hidden variable models deep into the cosmic history by utilizing the randomness in quasars of high redshift or even cosmic microwave background in future experiments. Further, we may find interesting applications in device-independent quantum information processing [21,32,60–66]. Scaling up the space-time extension in the local realism test is being actively pursued [67,68]. The same system may also help to examine the hypothesis for human free choice [3,6,8,53,69–72] and gravitational effect [73,74] and to address the collapse locality loophole [75–78].

Y. Zhang would like to thank E. Knill for the stimulating discussions about the PBR analysis method. This work has been supported by the National Key R&D Program of China (2017YFA0303900, 2017YFA0304000), National Fundamental Research Program, National Natural Science Foundation of China, and Chinese Academy of Sciences.

M-H. L., W. C. and Y. Z. contributed equally to this work.

*Note added.*—Recently, we become aware of a related work [79].

[1] A. Einstein, B. Podolsky, and N. Rosen, Phys. Rev. **47**, 777 (1935).
[2] J. Bell, Physics **1**, 195 (1964).
[3] J. S. Bell, *Speakable and Unspeakable in Quantum Mechanics: Collected Papers on Quantum Philosophy* (Cambridge University Press, Cambridge, England, 2004).
[4] J. F. Clauser, M. A. Horne, A. Shimony, and R. A. Holt, Phys. Rev. Lett. **23**, 880 (1969).

[5] J. F. Clauser and M. A. Horne, Phys. Rev. D **10**, 526 (1974).
[6] N. Brunner, D. Cavalcanti, S. Pironio, V. Scarani, and S. Wehner, Rev. Mod. Phys. **86**, 419 (2014).
[7] J.-Å. Larsson, J. Phys. A **47**, 424003 (2014).
[8] J. Kofler, M. Giustina, J.-A. Larsson, and M. W. Mitchell, Phys. Rev. A **93**, 032115 (2016).
[9] P. H. Eberhard, Phys. Rev. A **47**, R747 (1993).
[10] P. M. Pearle, Phys. Rev. D **2**, 1418 (1970).
[11] J. P. Jarrett, Noûs **18**, 569 (1984).
[12] S. J. Freedman and J. F. Clauser, Phys. Rev. Lett. **28**, 938 (1972).
[13] A. Aspect, P. Grangier, and G. Roger, Phys. Rev. Lett. **47**, 460 (1981).
[14] A. Aspect, P. Grangier, and G. Roger, Phys. Rev. Lett. **49**, 91 (1982).
[15] A. Aspect, J. Dalibard, and G. Roger, Phys. Rev. Lett. **49**, 1804 (1982).
[16] G. Weihs, T. Jennewein, C. Simon, H. Weinfurter, and A. Zeilinger, Phys. Rev. Lett. **81**, 5039 (1998).
[17] M. A. Rowe, D. Kielpinski, V. Meyer, C. A. Sackett, W. M. Itano, C. Monroe, and D. J. Wineland, Nature (London) **409**, 791 (2001).
[18] M. Ansmann, H. Wang, R. C. Bialczak, M. Hofheinz, E. Lucero, M. Neeley, A. O'connell, D. Sank, M. Weides, J. Wenner *et al.*, Nature (London) **461**, 504 (2009).
[19] J. Hofmann, M. Krug, N. Ortegel, L. Gérard, M. Weber, W. Rosenfeld, and H. Weinfurter, Science **337**, 72 (2012).
[20] M. Giustina, A. Mech, S. Ramelow, B. Wittmann, J. Kofler, J. Beyer, A. Lita, B. Calkins, T. Gerrits, S. W. Nam *et al.*, Nature (London) **497**, 227 (2013).
[21] B. G. Christensen, K. T. McCusker, J. B. Altepeter, B. Calkins, T. Gerrits, A. E. Lita, A. Miller, L. K. Shalm, Y. Zhang, S. W. Nam, N. Brunner, C. C. W. Lim, N. Gisin, and P. G. Kwiat, Phys. Rev. Lett. **111**, 130406 (2013).
[22] T. Scheidl, R. Ursin, J. Kofler, S. Ramelow, X.-S. Ma, T. Herbst, L. Ratschbacher, A. Fedrizzi, N. K. Langford, T. Jennewein *et al.*, Proc. Natl. Acad. Sci. U.S.A. **107**, 19708 (2010).
[23] B. Hensen, H. Bernien, A. E. Dréau, A. Reiserer, N. Kalb, M. S. Blok, J. Ruitenberg, R. F. Vermeulen, R. N. Schouten, C. Abellán *et al.*, Nature (London) **526**, 682 (2015).
[24] L. K. Shalm *et al.*, Phys. Rev. Lett. **115**, 250402 (2015).
[25] M. Giustina *et al.*, Phys. Rev. Lett. **115**, 250401 (2015).
[26] W. Rosenfeld, D. Burchardt, R. Garthoff, K. Redeker, N. Ortegel, M. Rau, and H. Weinfurter, Phys. Rev. Lett. **119**, 010402 (2017).
[27] E. Knill, Y. Zhang, and P. Bierhorst, arXiv:1709.06159.
[28] Y. Zhang, S. Glancy, and E. Knill, Phys. Rev. A **88**, 052119 (2013).
[29] Y. Zhang, S. Glancy, and E. Knill, Phys. Rev. A **84**, 062118 (2011).
[30] W. Zhang, L. You, H. Li, J. Huang, C. Lv, L. Zhang, X. Liu, J. Wu, Z. Wang, and X. Xie, Sci. China Phys., Mech. Astron. **60**, 120314 (2017).
[31] M. D. C. Pereira, F. E. Becerra, B. L. Glebov, J. Fan, S. W. Nam, and A. Migdall, Opt. Lett. **38**, 1609 (2013).
[32] Y. Liu, X. Yuan, M.-H. Li, W. Zhang, Q. Zhao, J. Zhong, Y. Cao, Y.-H. Li, L.-K. Chen, H. Li, T. Peng, Y.-A. Chen, C.-Z. Peng, S.-C. Shi, Z. Wang, L. You, X. Ma, J. Fan, Q. Zhang, and J.-W. Pan, Phys. Rev. Lett. **120**, 010503 (2018).
[33] See Supplemental Material at http://link.aps.org/supplemental/10.1103/PhysRevLett.121.080404 for detailed theoretical and experimental results.
[34] J. S. Bell and B. d'Espagnat, Prog. Sci. Culture **1/4**, 439 (1976).
[35] T. Maudlin, *Quantum Non-Locality and Relativity: Metaphysical Intimations of Modern Physics* (John Wiley & Sons, New York, 2011).
[36] L. Vaidman, Phys. Lett. A **286**, 241 (2001).
[37] J. Gallicchio, A. S. Friedman, and D. I. Kaiser, Phys. Rev. Lett. **112**, 110405 (2014).
[38] J. Handsteiner, A. S. Friedman, D. Rauch, J. Gallicchio, B. Liu, H. Hosp, J. Kofler, D. Bricher, M. Fink, C. Leung, A. Mark, H. T. Nguyen, I. Sanders, F. Steinlechner, R. Ursin, S. Wengerowsky, A. H. Guth, D. I. Kaiser, T. Scheidl, and A. Zeilinger, Phys. Rev. Lett. **118**, 060401 (2017).
[39] C. Wu, B. Bai, Y. Liu, X. Zhang, M. Yang, Y. Cao, J. Wang, S. Zhang, H. Zhou, X. Shi, X. Ma, J.-G. Ren, J. Zhang, C.-Z. Peng, J. Fan, Q. Zhang, and J.-W. Pan, Phys. Rev. Lett. **118**, 140402 (2017).
[40] C. Leung, A. Brown, H. Nguyen, A. S. Friedman, D. I. Kaiser, and J. Gallicchio, Phys. Rev. A **97**, 042120 (2018).
[41] J.-G. Ren, P. Xu, H.-L. Yong, L. Zhang, S.-K. Liao, J. Yin, W.-Y. Liu, W.-Q. Cai, M. Yang, L. Li *et al.*, Nature (London) **549**, 70 (2017).
[42] J. A. Stone and J. H. Zimmerman, http://emtoolbox.nist.gov/Wavelength/Edlen.asp (2011).
[43] J. H. Meeus, *Astronomical Algorithms* (Willmann-Bell, Incorporated, Richmond, VA, USA, 1991).
[44] F. Van Leeuwen, Astron. Astrophys. **474**, 653 (2007).
[45] K. M. Ferrière, Rev. Mod. Phys. **73**, 1031 (2001).
[46] F. C. Michel, Rev. Mod. Phys. **54**, 1 (1982).
[47] J. M. Cordes, J. M. Weisberg, D. A. Frail, S. R. Spangler, and M. Ryan, Nature (London) **354**, 121 (1991).
[48] T. L. Wilson and R. T. Rood, Annu. Rev. Astron. Astrophys. **32**, 191 (1994).
[49] M. A. Wayne, E. R. Jeffrey, G. M. Akselrod, and P. G. Kwiat, J. Mod. Opt. **56**, 516 (2009).
[50] C. A. Miller and Y. Shi, SIAM J. Comput. **46**, 1304 (2017).
[51] R. Arnon-Friedman, R. Renner, and T. Vidick, arXiv:1607.01797.
[52] M. J. W. Hall, Phys. Rev. A **84**, 022102 (2011).
[53] J. Barrett and N. Gisin, Phys. Rev. Lett. **106**, 100406 (2011).
[54] G. Pütz, D. Rosset, T. J. Barnea, Y.-C. Liang, and N. Gisin, Phys. Rev. Lett. **113**, 190402 (2014).
[55] A. Fine, Phys. Rev. Lett. **48**, 291 (1982).
[56] A. Peres, Found. Phys. **29**, 589 (1999).
[57] S. Popescu and D. Rohrlich, Found. Phys. **24**, 379 (1994).
[58] J. Barrett, N. Linden, S. Massar, S. Pironio, S. Popescu, and D. Roberts, Phys. Rev. A **71**, 022101 (2005).
[59] W. Hoeffding, J. Am. Stat. Assoc. **58**, 13 (1963).
[60] S. Pironio, A. Acín, S. Massar, A. B. de La Giroday, D. N. Matsukevich, P. Maunz, S. Olmschenk, D. Hayes, L. Luo, T. A. Manning *et al.*, Nature (London) **464**, 1021 (2010).
[61] P. Bierhorst, E. Knill, S. Glancy, A. Mink, S. Jordan, A. Rommal, Y.-K. Liu, B. Christensen, S. W. Nam, and L. K. Shalm, arXiv:1702.05178).
[62] R. Colbeck and R. Renner, Nat. Phys. **8**, 450 (2012).

[63] J. Barrett, L. Hardy, and A. Kent, Phys. Rev. Lett. **95**, 010503 (2005).
[64] S. Pironio, A. Acin, N. Brunner, N. Gisin, S. Massar, and V. Scarani, New J. Phys. **11**, 045021 (2009).
[65] U. Vazirani and T. Vidick, Phys. Rev. Lett. **113**, 140501 (2014).
[66] R. Gallego, L. Masanes, G. De La Torre, C. Dhara, L. Aolita, and A. Acín, Nat. Commun. **4**, 2654 (2013).
[67] J. Yin *et al.*, Science **356**, 1140 (2017).
[68] Y. Cao, Y.-H. Li, W.-J. Zou, Z.-P. Li, Q. Shen, S.-K. Liao, J.-G. Ren, J. Yin, Y.-A. Chen, C.-Z. Peng, and J.-W. Pan, Phys. Rev. Lett. **120**, 140405 (2018).
[69] M. J. W. Hall, Phys. Rev. Lett. **105**, 250404 (2010).
[70] D. Rideout, T. Jennewein, G. Amelino-Camelia, T. F. Demarie, B. L. Higgins, A. Kempf, A. Kent, R. Laflamme, X. Ma, R. B. Mann, E. Martn-Martnez, N. C. Menicucci, J. Moffat, C. Simon, R. Sorkin, L. Smolin, and D. R. Terno, Classical Quantum Gravity **29**, 224011 (2012).
[71] L. Hardy, in *Quantum [Un]Speakables II: Half a Century of Bell's Theorem*, edited by R. Bertlmann and A. Zeilinger (Springer International Publishing, Cham, Switzerland, 2017), p. 261.
[72] L. Hardy, arXiv:1705.04620.
[73] R. Penrose, Gen. Relativ. Gravit. **28**, 581 (1996).
[74] L. Disi, Phys. Lett. A **120**, 377 (1987).
[75] A. Kent, Phys. Rev. A **72**, 012107 (2005).
[76] D. Greenberger, K. Hentschel, and F. Weinert, *Compendium of Quantum Physics: Concepts, Experiments, History and Philosophy* (Springer Science+Business Media, Berlin, 2009).
[77] G. Manasseh, C. De Balthasar, B. Sanguinetti, E. Pomarico, N. Gisin, R. Grave De Peralta, and S. Gonzalez Andino, Front. Psychol. **4**, 845 (2013).
[78] P. Sekatski, N. Brunner, C. Branciard, N. Gisin, and C. Simon, Phys. Rev. Lett. **103**, 113601 (2009).
[79] D. Rauch, J. Handsteiner, A. Hochrainer, J. Gallicchio, A. S. Friedman, C. Leung, B. Liu, L. Bulla, S. Ecker, F. Steinlechner, R. Ursin, B. Hu, D. Leon, C. Benn, A. Ghedina, M. Cecconi, A. H. Guth, D. I. Kaiser, T. Scheidl, and A. Zeilinger, preceding Letter, Phys. Rev. Lett. **121**, 080403 (2018).